tvst

Article

Novel Dual-Targeting Antibody Fragment IDB0062 Overcomes Anti–Vascular Endothelial Growth Factor Drug Limitations in Age-Related Macular Degeneration

Seongbeom Kim[1], Gihong Min[1], Bomin Kim[1], Doseop Lee[1], Myongjae Lee[1], Jong-Hee Ko[1], and Hyuk-Sang Kwon[1]

[1] Research Laboratory, ILDONG Pharmaceutical Co., Ltd., Hwaseong-si, Korea

Correspondence: Hyuk-Sang Kwon, Research Laboratory, ILDONG Pharmaceutical Co., Ltd., 20, Samsung 1-ro 1-gil, Hwaseong-si 18449, Republic of Korea.
e-mail: hskwon@ildong.com

Received: May 26, 2021
Accepted: November 16, 2021
Published: December 30, 2021

Keywords: IDB0062; wAMD; non-responsiveness; alternative angiogenesis; bispecific antibody fragment; resistance

Citation: Kim S, Min G, Kim B, Lee D, Lee M, Ko JH, Kwon HS. Novel dual-targeting antibody fragment IDB0062 overcomes anti–vascular endothelial growth factor drug limitations in age-related macular degeneration. Transl Vis Sci Technol. 2021;10(14):35, https://doi.org/10.1167/tvst.10.14.35

Purpose: Repeated administration of anti–vascular endothelial growth factor drugs to treat age-related macular degeneration leads to resistance. To overcome this drawback, we developed the novel recombinant dual-targeting antibody fragment IDB0062, which is comprised of the anti–vascular endothelial growth factor A Fab and neuropilin 1-targeting peptide, and we assessed its properties.

Methods: We compared the in vitro activity of IDB0062 and conventional drugs using cell proliferation, wound healing, and Transwell assays. The in vivo efficacy of IDB0062 was determined using mouse choroidal neovascularization and oxygen-induced retinopathy models. To evaluate the ocular distribution of IDB0062, we intravitreally administered IDB0062 and ranibizumab to cynomolgus monkeys and measured the retinal drug levels.

Results: IDB0062 effectively inhibited not only vascular endothelial growth factor A in vitro but also placenta growth factor 2, vascular endothelial growth factor B, and platelet-derived growth factor BB, which induce vascular endothelial growth factor A–independent angiogenesis. In addition, IDB0062 showed non-inferior efficacy compared with aflibercept in vivo despite the low selectivity for mouse vascular endothelial growth factor A. In the monkey intravitreal pharmacokinetic study, IDB0062 improved drug distribution in the retina compared with ranibizumab, confirming the accelerated onset of pharmacological action when IDB0062 is injected in the vitreous humor.

Conclusions: Through neuropilin 1 binding, IDB0062 can improve the efficacy and accelerate the onset of pharmacological action in the posterior segment, which is targeted for macular degeneration, thereby improving drug responsiveness in drug-resistant patients.

Translational Relevance: Considering its novel mechanism of action, IDB0062 may help in controlling resistance to conventional anti–vascular endothelial growth factor drugs in clinical settings.

Introduction

Age-related macular degeneration (AMD) is a neurodegenerative disease that principally affects the macular region of the retina.[1,2] There are approximately 11 million AMD cases in the United States and 170 million cases globally.[2] AMD is the leading cause of visual disability in the industrialized world and the third leading cause of blindness globally.[2] Based on the observed pathophysiology, it is classified as wet AMD (wAMD) or dry AMD.[2] Wet AMD, also referred to as neovascular AMD, occurs when abnormal blood vessels from the choroid grow into the normally avascular subretinal pigment epithelium and subretinal regions.[2] Although neovascular AMD represents a small proportion of the total AMD cases, it is important to control this disease effectively because it accounts for most of the cases of blindness associated with AMD.[2]

Copyright 2021 The Authors

This work is licensed under a Creative Commons Attribution-NonCommercial-NoDerivatives 4.0 International License.

Downloaded from hwmaint.iovs.org on 04/25/2024

translational vision science & technology

High expression of vascular endothelial growth factor A (VEGFA) is a major factor that contributes to disease pathogenesis by stimulating choroidal neovascularization, resulting in the leakage of blood and fluid into the macula.[3] In the last decade, several intravitreal anti-VEGF drugs have been introduced; consequently, previously unachievable improvements in vision have been observed in patients with wAMD.[3] Ranibizumab (Lucentis) is the first approved recombinant humanized monoclonal antibody fragment that can block human VEGFA and improve visual acuity in patients with wAMD.[3] Early clinical trial data clearly demonstrated the benefits of ranibizumab; however, the mandatory monthly intravitreal injections place a significant burden on patients and healthcare systems. To resolve this issue, aflibercept (Eylea, a recombinant Fc fusion protein) and brolucizumab (Beovu), which require longer intervals between injections, were developed. The recently launched brolucizumab is a humanized single-chain variable fragment that inhibits VEGFA. It can be formulated at a 22-fold higher concentration than ranibizumab can be in terms of the molar ratio. Although the clearance rate of brolucizumab is comparable to that of other anti-VEGF drugs, the retention time may be prolonged as relatively abundant brolucizumab remains in the ocular tissue. Therefore, the dosing interval for brolucizumab could be up to 12 weeks, following an initial loading period. Although these anti-VEGF drugs have improved wAMD treatment significantly, some patients continue to show a poor response, are non-responsive to these agents, or experience a loss of efficacy over time after repeated administration.[4] There are several reasons for the development of resistance. One of the main mechanisms of resistance to anti-VEGF drugs is the generation of abnormal blood vessels in response to alternative proangiogenic factors, such as placental growth factor (PlGF), angiopoietins (ANGs), platelet-derived growth factor (PDGF), and hepatocyte growth factor (HGF), and the high expression of relevant receptors such as VEGFRs, Notch, and neuropilin 1 (NRP1).[5,6] Therefore, it is important to explore new targets for alternative angiogenesis to overcome drug resistance.

Neuropilins are multifunctional, single-pass transmembrane receptors that are highly expressed in endothelial cells, neurons, pancreatic islet cells, hepatocytes, and cancer cells.[8] Notably, NRPs were originally identified as co-receptors for the soluble class 3 semaphorins involved in axon guidance.[7] The two NRP family members, NRP1 and NRP2, are conserved among vertebrates and show approximately 40% similarity at the amino acid level with a conserved domain structure.[5] NRPs were identified as coreceptors for several members of the VEGF family. NRP1 interacts with VEGFA and VEGFR2 simultaneously, enhances signaling through this pathway, and promotes angiogenesis.[8] Moreover, NRP1 can participate in the angiogenic process by enhancing the signal cascade involving semaphorins, ANGs, PlGF, transforming growth factor β1 (TGF-β1), HGF, PDGF, and some fibroblast growth factors (FGFs).[9] Hence, NRP1/2 blockage on anti-VEGF drugs may increase their antiangiogenic efficacy, enabling them to overcome VEGFA resistance and improve responsiveness.[10]

Shin et al.[11] reported the development of an NRP1/2-specific, tissue-penetrating peptide (TPP; HTPGNSNKWKHLQENKKGRPRR) for the treatment of solid tumors. They demonstrated that when immunoglobulin G (IgG) was fused with TPP via an appropriate linker, paracellular permeability was improved, and the IgG could be efficiently distributed to the inner side of the solid tumor. TPP can be useful for improving the tissue permeability of its cargo protein. Therefore, improving the tissue permeability of TPP may be beneficial in the treatment of ophthalmic diseases. NRP1 is highly expressed in the posterior segment of the eyeball; consequently, if the distribution of ophthalmic drugs toward this segment can be improved by TPP, the drugs may be concentrated in the target tissue to promote the initiation of pharmacological action.

In this study, we aimed to construct an anti-VEGFA and anti-NRP1 dual-targeting antibody fragment (dubbed IDB0062) by the genetic fusion of an NRP1-targeting peptide to the C-terminus of the heavy and light chains of the anti-human VEGFA Fab and to evaluate the potential of IDB0062 as a candidate to overcome the drawbacks of anti-VEGF drugs.

Methods

Cells and Reagents

Primary human retinal microvascular endothelial cells (HRMECs), Complete Classic Medium with Serum and CultureBoost, and Complete Serum-Free Medium Kit with RocketFuel were purchased from Cell Systems (Kirkland, WA). Human umbilical vein endothelial cells (HUVECs) and F-12K medium were obtained from the American Type Culture Collection (Manassas, VA). Human coronary artery smooth muscle cells (HCASMCs), HCASMC conditioning medium, and human smooth muscle cell basal medium were acquired from Cell Applications (San Diego, CA).

translational vision science & technology

Downloaded from hwmaint.iovs.org on 04/25/2024

Human VEGFA and monkey NRP1 were obtained from Sinobiotech (Tianjin, China), and recombinant human VEGFA 165, PlGF2, VEGFB 167, PDGFBB, NRP1 ECD, and mouse NRP1 ECD were purchased from R&D Systems (Minneapolis, MN). Mouse and rabbit VEGFA were purchased from Kingfisher (Saint Paul, MN); anti-human kappa light chain Ab-horseradish peroxidase (HRP) from Sigma-Aldrich (St. Louis, MO); and ranibizumab and aflibercept from Roche (Basel, Switzerland) and Bayer (Leverkusen, Germany).

Animals

C57BL/6 mice were purchased from Koatech (Pyeongtaek, Korea) and maintained under a 12-hour dark/light cycle. Male and female drug-naïve cynomolgus monkeys were obtained from Covance Research Products (Alice, TX). All animals were acclimated to study conditions before dosing. Fresh food and water were provided daily, ad libitum. The care and treatment of all animals were in agreement with the ARVO Statement for the Use of Animals in Ophthalmic and Vision Research, and all procedures were performed in compliance with the Animal Welfare Act Regulations (9 CFR 3) and approved by the local Institutional Animal Care and Use Committee (18-626).

Protein Expression and Purification

The heavy and light chains of IDB0062 connected to two signal peptides (OmpA and PelB) were cloned into the pHEKA vector[12] at the BamHI/XhoI restriction enzyme sites. The construct was highly expressed in *Escherichia coli* SUPEX5 (KCTC12657BP, MC1601 mutant of derivative strain developed by B.-H. Cha at Gangwon University) after adding 0.1-mM isopropyl β-D-1-thiogalactopyranoside and incubating the cells for 20 hours. To harvest the expressed proteins efficiently, we added 0.1% (v/v) Triton X-100 into the culture broth after cell cultivation and incubated the broth for 4 hours at 20°C while gently stirring the broth. Next, we clarified the culture broth using a 0.45-µm filter and loaded the supernatant onto a Capto L affinity column (GE Healthcare, Chicago, IL) as the first step of purification. The eluate of the first purification step was loaded onto a HiTrap SP FF column (GE Healthcare) during the second purification step. Finally, the eluate was analyzed by 12% sodium dodecyl sulfate–polyacrylamide gel electrophoresis (SDS-PAGE) and size-exclusion high-performance liquid chromatography (SEC-HPLC; TSK-GEL G3000SWxL; Tosoh, Tokyo, Japan). We replaced the buffer with 10-mM histidine buffer and simultaneously concentrated the solution using a 10-kDa Amicon centrifugal filter (MilliporeSigma, Burlington, MA), until a concentration of 10 mg/mL was reached.

Surface Plasmon Resonance Spectroscopy for Determining the Binding Affinity of IDB0062

A surface plasmon resonance (SPR) assay was performed using a Biacore 2000 (GE Healthcare) system with an optimized CM5 sensor chip (GE Healthcare). Each antigen was immobilized onto a CM5 chip at 200 to 400 response units, and IDB0062 was diluted and injected into the VEGFA- or NRP1-coated chip at 3.12 to 200 nM. Kinetic parameters were determined using Biacore 2000 evaluation software (GE Healthcare)

HUVEC Proliferation Assay

We added 100 µL of HUVEC suspension containing 1.0×10^4 cells into each well of a 96-well plate along with F-12K medium containing 100 µg/mL heparin and 2% fetal bovine serum and incubated the plate at 37°C for 5 hours. Next, 100 ng/mL VEGFA was neutralized by incubation with either IDB0062 or ranibizumab (3 hours, 37°C) before cell treatment. The VEGFA–IDB0062/ranibizumab mixture was added into each well, and the plate was incubated (72 hours, 37°C). Cell proliferation was measured using the WST-1 assay kit (DoGenBio, Seoul, Korea), according to the manufacturer's protocol.

Wound Healing Assay

Primary HRMECs were seeded in six-well plates (5×10^4 cells/well), incubated in complete classic medium with supplements included in the media kit (Cell Systems) for 3 days, and then subjected to serum starvation using complete serum-free medium (CSFM) for 6 hours. Thereafter, a straight scratch was made across the layer of cultured cells using a 200-µL micropipette tip. The cells were treated with ranibizumab, aflibercept, or IDB0062 in the presence or absence of VEGFA (50 ng/mL), VEGFB (50 ng/mL), or PlGF2 (100 ng/mL) in CSFM and incubated (37°C, 5% CO_2). Images of the cells were acquired using an Eclipse TE2000-U inverted fluorescence microscope (Nikon, Tokyo, Japan) at 0 hour and at the final time point (15.5–16.5 hours). The wound area was quantitated using the MRI Wound

translational vision science & technology

Downloaded from hwmaint.iovs.org on 04/25/2024

Healing Tool of ImageJ (v1.4.3.67; National Institutes of Health, Bethesda, MA). Half-maximal inhibitory concentration (IC_{50}) was calculated using the Prism program (GraphPad, San Diego, CA).

HCASMC Transwell Migration Assay

HCASMCs were seeded (5.4×10^4 cells/well) in 2% gelatin-coated upper chambers of Transwell plates in 100 µL of serum-free medium containing 0.5, 1, or 3 µM IDB0062, 1 or 3 µM ranibizumab, or 1 or 3 µM aflibercept. In the lower chambers, 600 µL of serum-free medium containing 30 ng/mL PDGF-BB with each of the above drugs was added. After incubation (3 hours, 37°C), the cells on the lower surface of the membrane were stained with hematoxylin and eosin and analyzed using an Eclipse TE2000-U microscope. Image analysis was performed using ImageJ, with the following analytical conditions: area range, 1 to 40,000 pixels; RGB filter setting, 26_50_0.

NRP1 Internalization

HRMECs (5×10^4) stabilized in an eight-well plate for 24 hours were treated with serum-free medium containing 1 µM IDB0062 or ranibizumab at 4°C and 37°C for 1 hour. To determine IDB0062 and ranibizumab levels on the cell surface or in the intracellular space, the cells were stained with Alexa Fluor 488–Conjugated Goat anti-Human IgG antibody (A11013; Thermo Fisher Scientific, Waltham, MA) for 1 hour at 25°C ± 2°C. NRP1 was stained with Recombinant Anti-NRP1 antibody (ab81321; Abcam, Cambridge, MA) and Alexa Fluor 594–Conjugated Goat anti-Rabbit IgG antibody (A11037; Thermo Fisher Scientific) for 1 hour at room temperature. Images were acquired using an LSM800 confocal microscope (Carl Zeiss Microscopy, White Plains, NY).

Establishment of a Laser-Induced Choroidal Neovascularization Mouse Model

Laser photocoagulation was performed using a customized indirect head-set delivery system (Ilooda, Suwon, Korea) at 3, 6, 9, and 12 o'clock positions of the retina at two-disc diameters from the optic disc. The laser parameters were as follows: spot size, 200 µm; power, 250 mW; and exposure time, 100 ms. On day 4 after laser photocoagulation, the vehicle (i.e., the buffer alone, without IDB0062), IDB0062 (0.2 µM or 1 µM), or aflibercept (1 µM) was injected into the vitreous cavity of mice (n = 12). Three days later, the retinal pigment epithelium–choroid–scleral complexes were immunostained using isolectin-B4 (1:100; Life Technologies, Carlsbad, CA). The choroidal neovascularization (CNV) area was measured using ImageJ.

Establishment of an Oxygen-Induced Retinopathy Mouse Model

Oxygen-induced retinopathy (OIR) was induced in newborn mice by exposing the mice to hyperoxia (75% O_2) for 5 days from postnatal day P7 to P12.[13] On P14, the vehicle, IDB0062 (0.2 µM or 1 µM), or aflibercept (1 µM) was injected into the vitreous cavity of each mouse (n = 12). On P17, the retinal tissues were immunostained with isolectin B4 (1:100). The neovascular tuft area was measured using ImageJ.

Determination of the Ocular Distribution of IDB0062 After Intravitreal Administration in Cynomolgus Monkeys

The dosage of each drug is shown in Table 1. Bolus intravitreal injections containing each of the molecules were administered at a dose of 50 µL into each eye by a veterinary ophthalmologist. Immediately after intravitreal injection on day 0, the retinal tissues were collected from the designated animals at the indicated time points (Table 2). At the time of euthanasia, both eyes were enucleated and stored at –70°C. Within 2 days, the retinal tissues were collected and weighed, and the IDB0062 concentrations were determined using the Fab enzyme-linked immunosorbent assay. Samples were loaded in the wells of a 96-well plate coated with human VEGFA. HRP-conjugated anti-human kappa light chain antibody was used as a detection antibody. Noncompartmental analysis was used for the composite retina to obtain data regarding the IDB0062 and ranibizumab concentrations.

Statistical Analysis

Data are reported as the mean ± standard error of the mean, unless specified otherwise. Means were compared using the one-way analysis of variance (ANOVA) with Bonferroni's post hoc tests. All tests were conducted using Prism software. Results with $P < 0.05$ were considered statistically significant.

translational vision science & technology

Downloaded from hwmaint.iovs.org on 04/25/2024

Table 1. Treatment Groups

Group	Animals, *n*		Test Drug	Dose Route	Target Dose Level (µg/eye)	Target Dose Volume (µL/eye)	Samples Collected
	Male	Female					
1	4	4	IDB0062	IVT (OD)	300	50	Retina
2	6	0	Ranibizumab	IVT (OD)	500	50	Retina

IVT, intravitreous; OD, right eye.

Table 2. Sampling Time Points in the Pharmacokinetic Study Involving Cynomolgus Monkeys

Time Point (h)	Group 1 (300 µg/Eye IDB0062)	Group 2 (500 µg/Eye Ranibizumab)
6	1 male	1 male
24	1 female	1 male
48	1 male	1 male
96	1 female	1 male
168	1 male	1 male
240	1 female	1 male
336	1 male	—
504	1 female	—

Results

IDB0062 Preparation, Molecular Structure, and Characteristics

IDB0062 is a new biological entity containing a TPP at the C-terminus of the anti-VEGFA Fab molecule (Fig. 1A). To increase production efficiency, we substituted the cysteine residues in the heavy and light chains (C226S, C214S), according to the procedure described by Kang et al.[12] The Fab portion of IDB0062 has the same amino acid sequence as ranibizumab, including the complementarity-determining region, except that there is no disulfide bond between the heavy chain and the light chain. When IDB0062 and ranibizumab were produced in SUPEX5 using the same procedure and purified using Capto L affinity resin, different patterns were observed in the spectrum of size-exclusion chromatography (Fig. 1B). Only the third ranibizumab peak indicated VEGFA-binding activity (data not shown), whereas the entire IDB0062 peak exhibited VEGFA-binding activity. Thus, these point mutations may have resulted in an increased production efficiency of IDB0062 and simplified the purification process compared with the production efficiency and purification process of ranibizumab.

Highly purified IDB0062 was obtained via a two-step purification process involving Capto L affinity and cation exchange chromatography and was identified by SDS-PAGE analysis. Due to the lack of inter-disulfide bonds, IDB0062 was detected as two bands that were approximately 28 kDa under non-reducing conditions, in contrast to ranibizumab (Fig. 1C). SEC-HPLC confirmed that the purity of IDB0062 was almost higher than 95% (Fig. 1D). Thus, these data revealed that IDB0062 existed in the heterodimeric form with heavy and light chains, without any inter-chain disulfide bonds. The stability of IDB0062 was well maintained even though there was no disulfide bond between the heavy chain and the light chain. (See Supplementary Fig. S1 for a long-term stability study of IDB0062 that was performed by VEGFA/NRP1 ELISA assay.)

SPR Spectroscopy to Determine the Binding Affinity of IDB0062

Compared with previous findings regarding ranibizumab,[14] the binding affinity (K_D) of IDB0062 to human VEGFA was approximately 67 pM, and the value was similar to that of ranibizumab (Fig. 1E). This implies that the tertiary structure of IDB0062 was well maintained in the absence of inter-disulfide bonds. As ranibizumab showed a relatively lower binding affinity to rodent VEGFA,[15,16] the K_D values of IDB0062 for mouse and rabbit VEGFA were relatively lower than that for human VEGFA; the K_D values of IDB0062 were 5.24 nM in mouse VEGFA and 11.1 µM in rabbit VEGFA (Fig. 1E). In contrast, the K_D values of IDB0062 for human, monkey, and mouse NRP1 were 52.5, 25.8, and 37.1 nM, respectively. The

translational vision science & technology

Downloaded from hwmaint.iovs.org on 04/25/2024

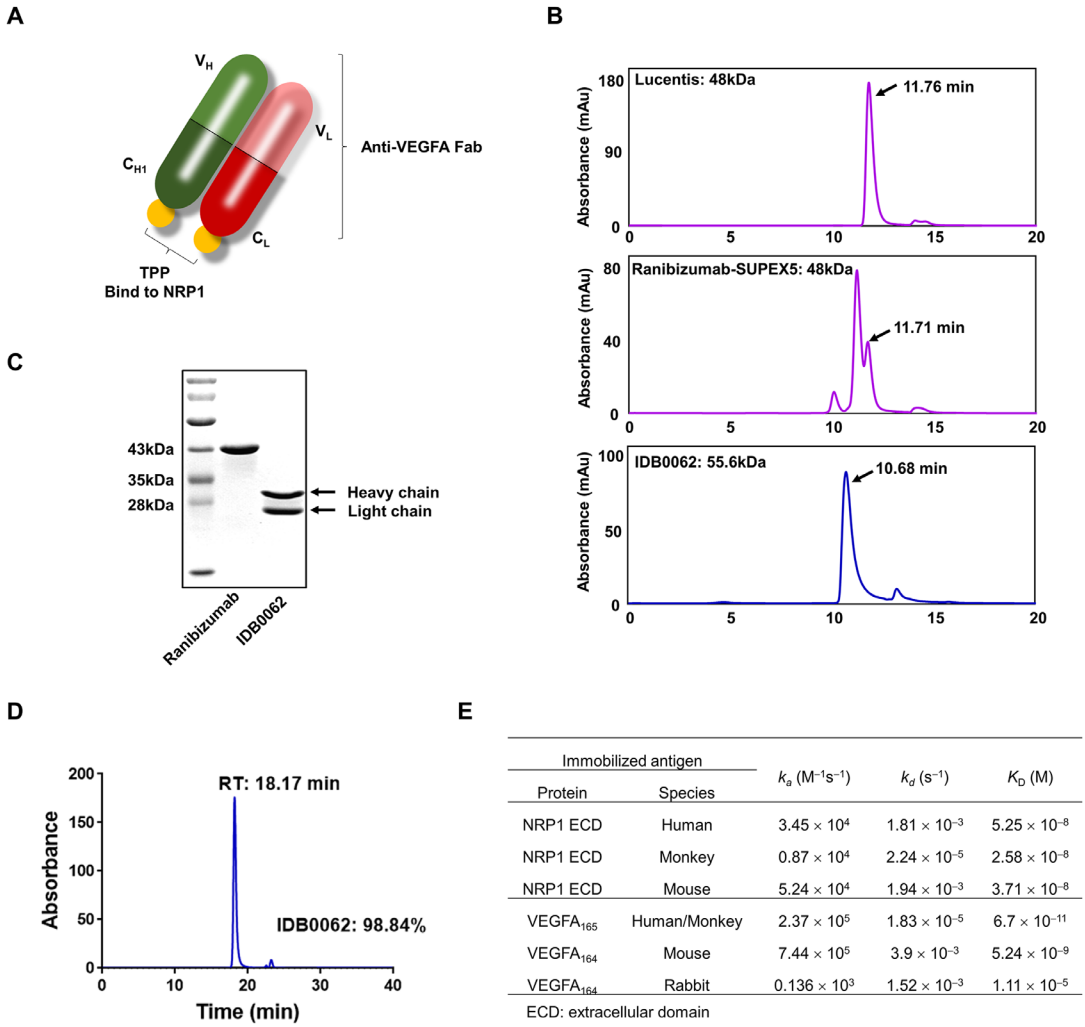

Immobilized antigen		k_a ($M^{-1}s^{-1}$)	k_d (s^{-1})	K_D (M)
Protein	Species			
NRP1 ECD	Human	3.45×10^4	1.81×10^{-3}	5.25×10^{-8}
NRP1 ECD	Monkey	0.87×10^4	2.24×10^{-5}	2.58×10^{-8}
NRP1 ECD	Mouse	5.24×10^4	1.94×10^{-3}	3.71×10^{-8}
$VEGFA_{165}$	Human/Monkey	2.37×10^5	1.83×10^{-5}	6.7×10^{-11}
$VEGFA_{164}$	Mouse	7.44×10^5	3.9×10^{-3}	5.24×10^{-9}
$VEGFA_{164}$	Rabbit	0.136×10^3	1.52×10^{-3}	1.11×10^{-5}

ECD: extracellular domain

Figure 1. Production of IDB0062 in *E scherichia coli* (SUPEX5) cells and characterization. (A) Schematic diagram of IDB0062 showing TPPs recombinantly linked to the C-terminus of each of the heavy and light chains via the $(G_4S)_3$ linker. (B) SEC-HPLC of the Capto L eluate of each clone. Ranibizumab expressed in SUPEX5 cells (ranibizumab-SUPEX5) showed several peaks in Capto L eluate when compared with IDB0062. (C) IDB0062 was analyzed by SDS-PAGE under non-reducing conditions and compared with ranibizumab. Due to the lack of disulfide bonds between the heavy and light chains, IDB0062 was detected as two bands (*black arrows*) under non-reducing conditions. The two arrows indicate the heavy and light chains of IDB0062. M, markers; lane 1, ranibizumab; lane 2, IDB0062. (D) The purity of IDB0062 was determined after a two-step purification process using SEC-HPLC (Tosoh TSKgel G3000SWXL; 0.2 M KPi, 0.25 M KCl, pH 6.2, 40 minutes). The purity of the eluate obtained after the second purification step was >95%. (E) Binding affinity of IDB0062 to VEGFA and NRP1 based on Biacore 2000 analysis.

NRP1-binding affinity of IDB0062 is well conserved in various species, and we confirmed that the use of monkey and mouse species would be appropriate for performing pharmacological and pharmacokinetic studies of IDB0062.

NRP1-Internalizing Efficacy of IDB0062

Shin et al.[11] reported that TPP-linked Fc increases the vascular and paracellular permeability via the induction of NRP1 internalization following binding to NRP1. To confirm whether IDB0062 could cause the internalization of NRP1 into the cytoplasm, we conducted confocal microscopy analysis. When IDB0062 was incubated with NRP1-highly expressing HRMECs for 1 hour at 4°C, most of the IDB0062 was located on the cell surface with NRP1. However, when we incubated HRMECs with IDB0062 for 1 hour at 37°C, both IDB0062 and NRP1 were internalized into the cytoplasm and formed foci (Fig. 2). When the drug was washed out and the HRMECs were incubated for 24 hours under the same conditions, the foci disappeared and the degree of colocalization with NRP1 fell to the level of the control HRMECs and ranibizumab-treated HRMECs. In other words, it was confirmed that the foci formed due to the binding of IDB0062

translational vision science & technology

Downloaded from hwmaint.iovs.org on 04/25/2024

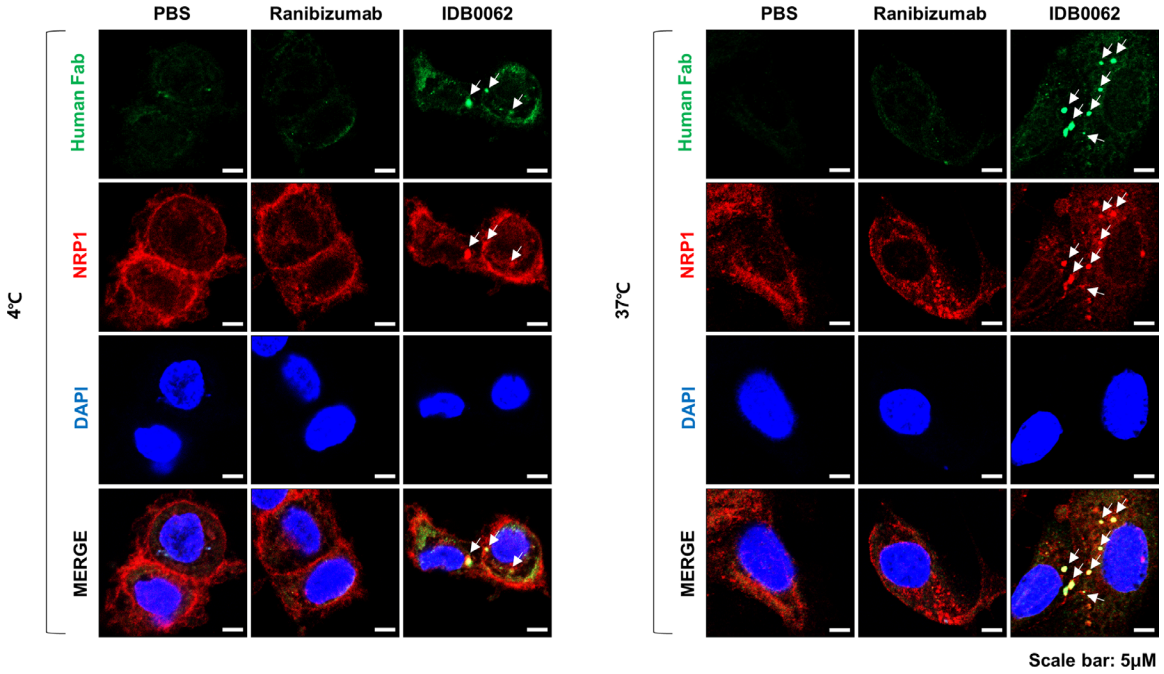

Figure 2. Evaluation of NRP1 internalization in HRMECs. IDB0062 binds to NRP1 expressed on the cell surface. After incubation with HRMECs at 37°C for 1 hour, the IDB0062 (*green*)–NRP1 (*red*) complex was internalized in the cytoplasm and formed foci (*yellow*, indicated with *white arrows*). HRMECs were treated with IDB0062 (1 μM) or ranibizumab (1 μM). Nuclei were counterstained with DAPI. In the microscopic fields, $n = 10$.

and NRP1 disappeared after the drug was washed out and the cell surface was restored to the original state (see Supplementary Fig. S2 for the results of the confocal analysis). In contrast, ranibizumab did not bind to NRP1; no signals were observed in the cytoplasm even after incubating the cells at 37°C for 1 hour. Thus, we confirmed that IDB0062 can colocalize with NRP1 in the cytoplasm under physiological conditions.

Cell-Based Assays to Determine IDB0062 Activity

Using cell-based assays, we determined whether IDB0062 could suppress VEGFA-, VEGFB-, PlGF2-, and PDGFBB-induced biological responses, and we compared our results with those of ranibizumab and aflibercept. To assess this further, we performed three different in vitro studies. First, we performed the human VEGFA-induced HUVEC proliferation assay to determine the inhibitory effect of IDB0062. When HUVECs were treated with 100 ng/mL VEGFA, cell proliferation significantly increased by approximately threefold or more compared with that in the control group. However, when 10 nM IDB0062 or ranibizumab was incubated with VEGFA at 37°C for 3 hours, VEGFA-induced cell proliferation was effectively suppressed to the control level in both groups (Fig. 3A).

Second, to confirm the antiangiogenic role of TPP against several growth factors, we performed a wound healing assay (Fig. 3B). After creating a wound on an HRMEC monolayer, cell migration was induced by treating the cells with VEGFA, VEGFB, or PlGF2. We then treated cells with IDB0062, ranibizumab, or aflibercept and evaluated the cell migration. The suppression of VEGFA-induced migration in response to IDB0062 treatment was comparable to that observed in response to ranibizumab and aflibercept treatment. The IC_{50} against VEGFA was similar for ranibizumab, aflibercept, and IDB0062 (Fig. 3C). VEGFB- or PlGF2-induced migration was blocked by IDB0062 or aflibercept but not by ranibizumab. The IC_{50} of IDB0062 for PlGF2 and VEGFB was similar to that of aflibercept (Fig. 3C).

Third, we performed a Transwell assay using HCASMCs, as these primary cells exhibit very low VEGF receptor expression and relatively high expression of both NRP1 and PDGF receptors.[17] We evaluated the effect of IDB0062 on HCASMC migration induced by interactions between PDGFBB and PDGFR. In the negative control group treated with PDGFBB alone, HCASMC migration was approximately seven times higher than that in the control group (Fig. 4A). When PDGFBB-treated HCASMCs were exposed to ranibizumab, migration

translational vision science & technology

Downloaded from hwmaint.iovs.org on 04/25/2024

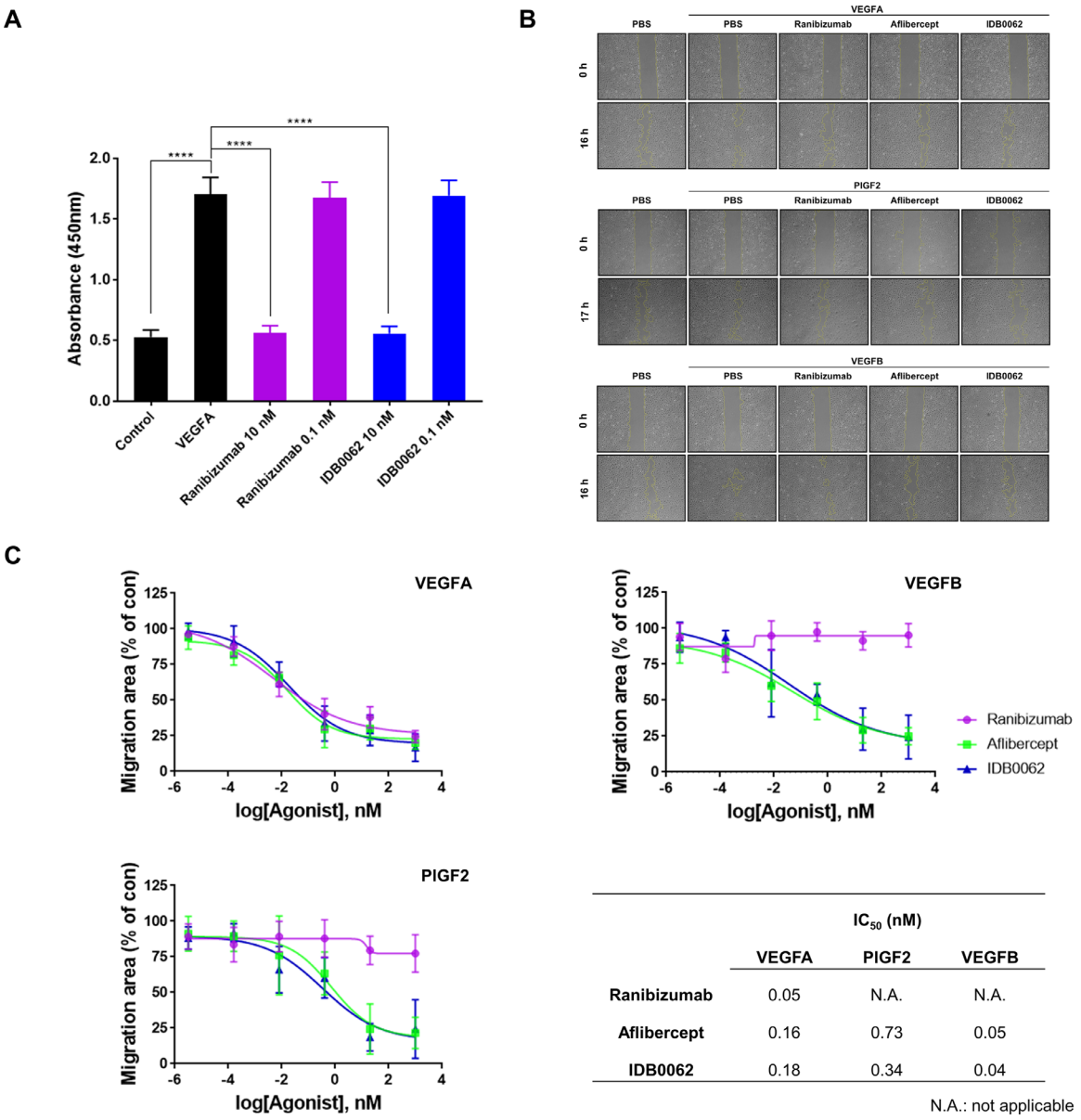

	IC$_{50}$ (nM)		
	VEGFA	PIGF2	VEGFB
Ranibizumab	0.05	N.A.	N.A.
Aflibercept	0.16	0.73	0.05
IDB0062	0.18	0.34	0.04

N.A.: not applicable

Figure 3. Evaluation of the inhibitory effect of IDB0062 on angiogenesis. (A) The inhibitory effect of IDB0062/ranibizumab on VEGFA-induced HUVEC proliferation was measured. There was no difference in the level of inhibition of HUVEC proliferation between IDB0062 and ranibizumab. (B) Wound healing assay to compare the inhibitory effects of IDB0062, ranibizumab, and aflibercept using HRMECs under the same conditions in which several growth factors were used to induce cell migration. (C) The IC$_{50}$ values for each drug are summarized. IDB0062 inhibited angiogenesis induced by not only VEGFA but also VEGFB and PlGF2.

was promoted in a manner similar to that observed in the negative control. In contrast, IDB0062 and aflibercept effectively inhibited PDGF-BB–induced HCASMC migration (Figs. 4A, 4B). A previous study[18] has shown that aflibercept may directly bind to PDGFBB because it contains the third domain of VEGFR2. However, as IDB0062 cannot directly bind to PDGF-BB (see Supplementary Table S1 for the binding affinity of IDB0062 to PDGF-BB), we can conclude that the inhibition of HCASMC migration to a level similar to that of aflibercept is responsible for the binding of TPP to NRP1.

IDB0062 Antiangiogenesis Activity in Mouse CNV and OIR Models

To evaluate and compare the efficacy of IDB0062 during pathological neovascularization with that of aflibercept in the retina and choroid, we used laser-induced CNV and OIR models. In the mouse CNV study, the CNV area was measured 4 days after laser treatment. The reduction in the CNV area was measured after the intravitreal (IVT) administration of 1 μM aflibercept or two concentrations of IDB0062 (0.2 and 1 μM) in CNV mice. The CNV area was

translational vision science & technology

Downloaded from hwmaint.iovs.org on 04/25/2024

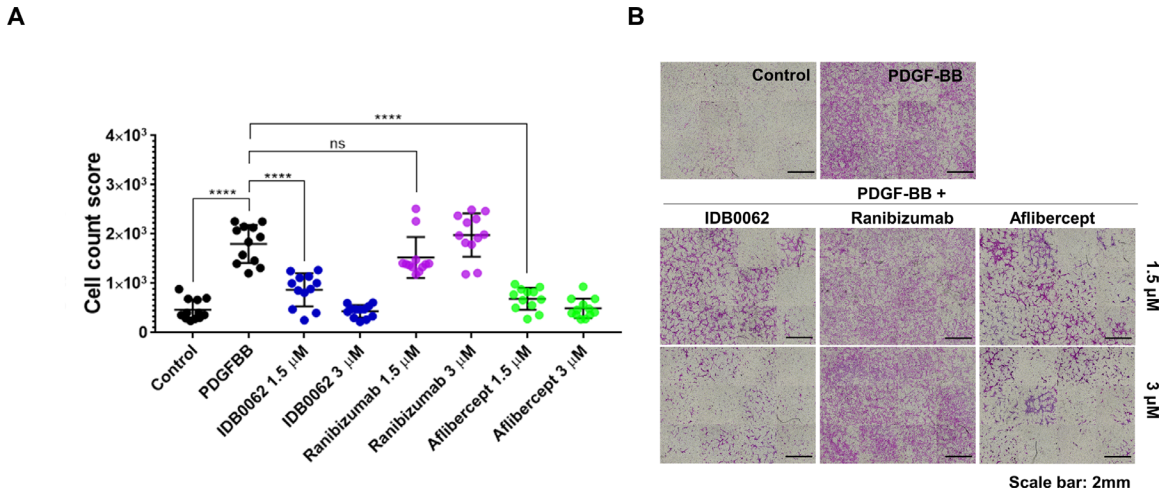

Figure 4. Evaluation of the inhibitory effect of IDB0062 on PDGF-BB–induced cell migration. (A) Transwell assays were conducted using HCASMCs to evaluate the efficacy of IDB0062, ranibizumab, and aflibercept in inhibiting PDGF-BB–induced cell migration. Cells were counted in 12 random fields. The number of migrated cells in the IDB0062- or aflibercept-treated groups decreased in a concentration-dependent manner. In contrast, ranibizumab did not exhibit an inhibitory effect. The data are presented as the mean ± standard deviation based on the results of three independent experiments. (B) Cells that had migrated to the lower chambers of Transwell plates were fixed and stained with hematoxylin and eosin.

significantly reduced in the aflibercept- and IDB0062-treated groups compared with that in the vehicle group (Fig. 5A). Aflibercept and IDB0062 showed similar CNV inhibitory efficacies.

Recently, the OIR model was used to define the function of NRP1 and its ligands in retinal neovascularization because NRP1 is expressed in both endothelial and retinal pigment epithelial cells.[19] Consistent with the results obtained using the CNV model, IDB0062 significantly reduced neovascularization compared with the vehicle, and the results were not significantly different from those for aflibercept (Fig. 5B).

As the above two models are disease models that reflect inflammation-induced angiogenesis in which VEGFA is dominant, they might not be suitable for proving the superior efficacy of IDB0062 in terms of inhibiting the VEGFA-independent angiogenic pathway. Moreover, IDB0062 achieved inhibition comparable to that of aflibercept despite its relatively lower affinity for mouse VEGFA, suggesting that VEGFA-independent activities contribute to this observed effect.

Ocular Distribution of IDB0062 in Cynomolgus Monkeys

Macular degeneration occurs in the posterior segment that includes retina and choroid; however, most commercially available macular degeneration drugs such as ranibizumab, aflibercept, and brolucizumab are injected intravitreally. As a result, the drugs may not exert their therapeutic effects directly at the disease site. As the expression of VEGFA is high in the CNV membrane of patients with AMD,[20] an improvement in drug distribution in the posterior segment is necessary for achieving sufficient levels of efficacy. Most of the drugs administered intravitreally diffuse from the vitreous humor to the posterior compartment before being delivered to the target tissue, where they exert their effects. TPP–NRP1 binding possibly improved the efficacy of IDB0062 through a novel mechanism of action. Additionally, it could also play an important role in enhancing paracellular permeability to facilitate drug penetration into target tissues. Hence, the administration of IDB0062 into the vitreous humor could improve drug distribution in the ocular tissues. To assess this aspect, we evaluated the ocular distribution of IDB0062 by administering a single intravitreal dose in cynomolgus monkeys. We collected the retinal tissues at determined time points (Table 2) after drug administration. The group designation, number of animals, target dose levels, and target dose volumes are listed in Table 1.

The pharmacokinetic profiles of IDB0062 and ranibizumab in the retina are described in Figure 6. After reaching maximum concentration (C_{max}), the drug concentration declined; the half-life ($t_{1/2}$) in the retina was 53.3 hours for IDB0062, and the $t_{1/2}$ was 67.6 hours for ranibizumab (Fig. 6C). The C_{max} in the retinal tissue of the IDB0062-treated group (142 μg/mL)

translational vision science & technology

Downloaded from hwmaint.iovs.org on 04/25/2024

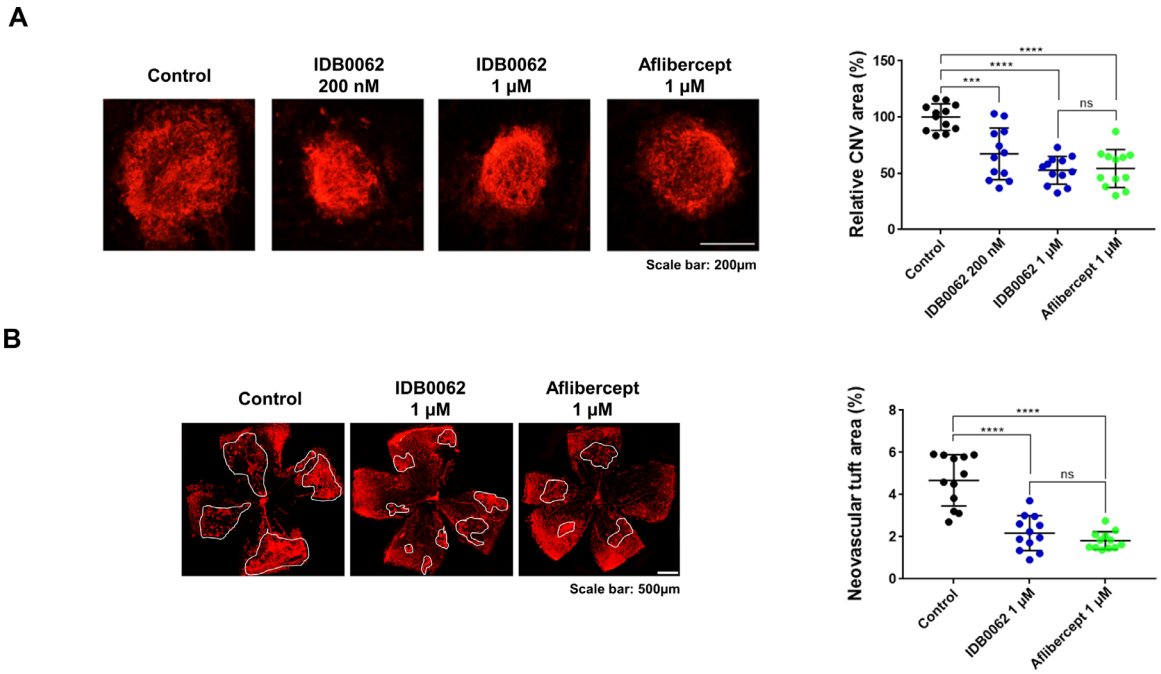

Figure 5. Evaluation of the antiangiogenic effects of IDB0062 in two in vivo mouse models. (A) The efficacy of IDB0062 in reducing the CNV area was evaluated using a mouse CNV model. Images were acquired by microscopy and a customized laser indirect ophthalmoscope system. IDB0062 and aflibercept significantly reduced the CNV area compared with the negative control. CNV area was measured using ImageJ. (B) OIR was induced in newborn mice using a closed chamber under hyperoxia (75% ± 0.5% O_2) conditions for 5 days from postnatal day P7 to P12. At P14, the vehicle, IDB0062, or aflibercept was injected into the vitreous cavity of mice. At P17, the eyes were prepared for immunostaining whole-mounted retinas with isolectin B4 (1:100). IDB0062 significantly reduced neovascularization compared with the vehicle, and the findings were not significantly different from those for aflibercept. Neovascular areas were quantitatively analyzed by outlining neovascular tufts (solid white line) using Adobe Photoshop and measuring the area using ImageJ.

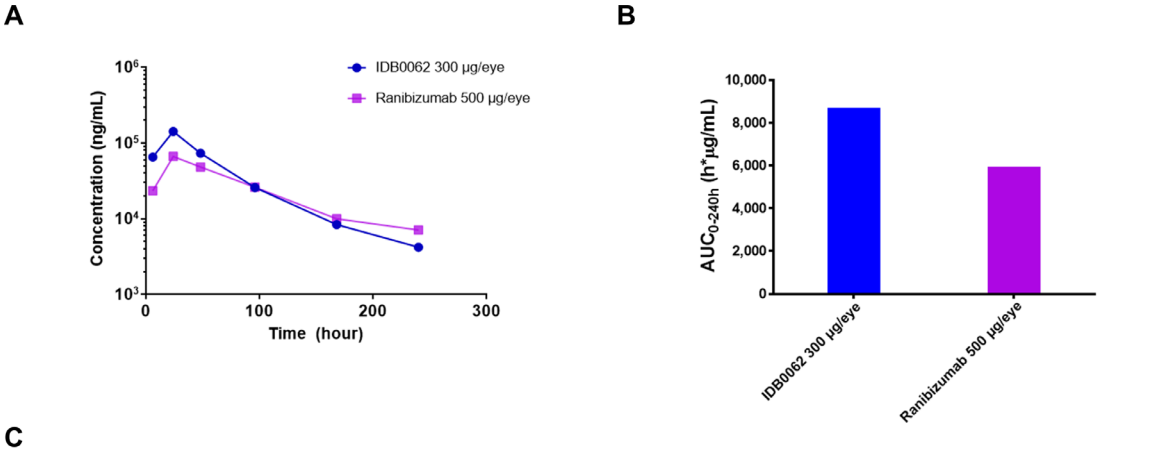

C

Drug	Dose	Matrix	Eye	Sex	C_{max} (μg/mL)	T_{max} (h)	AUC_{240} (day·μg/mL)	$T_{1/2}$ (h)
IDB0062	300 μg/eye	Retina	OD	M/F	142	24	362.9	53.3
Ranibizumab	500 μg/eye	Retina	OD	M	66.2	24	247.1	67.6

OD, right eye

Figure 6. (A) Hour–concentration profiles of IDB0062 and ranibizumab in the retinal tissue of cynomolgus monkeys following intravitreal injection. (B) *Bars* represent the value of AUC_{0-240} after the single administration of either IDB0062 or ranibizumab. (C) Pharmacokinetic parameters of IDB0062 and ranibizumab.

translational vision science & technology

Downloaded from hwmaint.iovs.org on 04/25/2024

was approximately 2.1-fold higher than that of the ranibizumab-treated group (66.2 μg/mL), whereas the area under the curve (AUC) in the retinal tissue in the IDB0062-treated group (362.9 d·μg/mL) was approximately 1.5-fold higher than that of the ranibizumab-treated group (247.1 d·μg/mL) (Fig. 6C). Although based on a low number of animals, our data suggest that IDB0062 exhibits a better retinal distribution than ranibizumab, even at a lower injected dose. Thus, an improvement in pharmacological activity can be expected with a smaller dose. This provides an opportunity to improve drug safety by injecting smaller doses, thereby improving the therapeutic potential and extending the administration cycle.

Discussion

Patients with wAMD can lose their central vision after the formation of abnormal blood vessels that grow into the subretinal region. Several studies have reported that blocking VEGFA can slow or stop disease progression, as VEGFA is the most important factor that causes abnormal blood vessel growth and vessel leakage.[21] Therefore, ranibizumab, which can effectively inhibit VEGFA, is widely used as a treatment for macular degeneration based on the abundant safety data available.

Anti-VEGF drugs such as ranibizumab show substantial visual improvement by effectively scavenging VEGFA; therefore, they act as a driving force for the growth of the AMD market. However, patient convenience must be improved by extending the administration interval and enhancing drug efficacy to improve vision in these patients, as this is the most important but currently unmet medical need in AMD treatment. Ranibizumab improves visual acuity in the early stages of development; however, the administration interval is relatively short. Therefore, patients have to visit the hospital frequently; moreover, frequent administration may raise safety issues. Therefore, drugs with administration interval extended to 2 or 3 months, such as aflibercept and brolucizumab, have been developed, leading to somewhat improved patient convenience. However, as the drugs developed so far are based on a common mechanism to inhibit VEGFA, there is a limit to improving their efficacy. In fact, if these anti-VEGF drugs are repeatedly administered for a long time, resistance or non-responsiveness to anti-VEGF drugs increases, leading to a gradual decrease in visual acuity improvement. Considering that macular degeneration has to be treated and managed for a long time, the decrease in drug responsiveness due to frequent administration is a challenge that must be overcome. Therefore, candidates with a novel mechanism of action are being actively developed.

In our current study, IDB0062 was prepared by linking a TPP targeting NRP1 to the C-terminus of the anti-VEGF Fab. We tried to evaluate the beneficial aspects of NRP1 binding property of IDB0062. First, considering that NRP1 acts as a co-receptor that enhances the response of several types of growth factors, it may play an important role in inducing and enhancing VEGFA-independent alternative angiogenesis in pathological conditions. Thus, we evaluated the inhibitory potential against various growth factors that IDB0062 cannot directly bind to, such as VEGFB, PlGF2, and PDGFBB, using the wound healing assay. When PlGF2 and VEGFB were mixed with various concentrations of ranibizumab, aflibercept, and IDB0062 and then treated with HRMEC to compare the inhibitory activity, ranibizumab did not show any inhibitory effect; in contrast, IDB0062 showed inhibitory effect similar to that of aflibercept. Aflibercept incorporates the second binding domain of VEGFR1 and the third domain of VEGFR2, fused with the Fc segment of a human IgG backbone.[22] Therefore, it can directly scavenge both VEGFB and PlGF2 immediately. In contrast, IDB0062 directly binds to only VEGFA. The inhibitory effect of IDB0062 is considered comparable to that of aflibercept, because the TPP of IDB0062 inhibited the possibility of NRP1-mediated alternative angiogenesis by binding to it. In addition, in the migration assay using HCASMC, IDB0062 effectively inhibited the PDGFBB-induced migration, similar to aflibercept. Although we could not obtain direct evidence that IDB0062 is superior to aflibercept, available scientific literature suggests that growth factors not targeted by aflibercept, such as FGF2, TGF-β, VEGFC, and VEGFD, may be sufficiently suppressed by IDB0062. These properties provide the possibility of overcoming resistance and non-responsiveness to anti-VEGF drugs by effectively inhibiting angiogenesis in which NRP1 is involved, thereby enhancing the efficacy of IDB0062 substantially compared with existing anti-VEGF drugs.

Second, compared with ranibizumab, it was confirmed that IDB0062 can be distributed relatively more abundantly in the posterior segment of the eye where NRP1 is highly expressed. Among the eye tissues, the posterior segment containing the retina and choroid has relatively abundant neurons and endothelial cells; therefore, the expression of NRP1 is also high. As IDB0062 binds specifically to NRP1 when administered intravitreally, it can be distributed more predominantly in the posterior segment of the eye

translational vision science & technology

Downloaded from hwmaint.iovs.org on 04/25/2024

where NRP1 is highly expressed. In the monkey intravitreal pharmacokinetic study using ranibizumab as the control group, IDB0062 showed a 1.5-fold higher C_{max} in the retina and better AUC than ranibizumab, despite being administered at a lower dose. Currently, most biopharmaceuticals used to treat AMD have a loading phase, where the drug is injected monthly for 3 months. This is done to ensure drug efficacy (improving vision) by increasing the initial concentration of the drug in the target tissue. Thereafter, the drug is repeatedly administered in a cycle to maintain its concentration. The tissue distribution property of IDB0062, which we confirmed in the intravitreal pharmacokinetic study, can increase the drug concentration in the target tissue within a short period and reduce the time required for the onset of pharmacological action, which in turn eliminates the initial loading phase of treatment and can also reduce the number of dosing and treatments. It is a novel characteristic that can satisfy the unmet needs of improving patient convenience and improving drug efficacy.

In conclusion, our study revealed that TPP, a novel peptide that targets NRP1, can confer new functions on anti-VEGF drugs in terms of enhancing the efficacy and improving the tissue distribution of drugs. These findings indicate that IDB0062 can be a new alternative that can overcome the shortcomings of various anti-VEGF drugs currently in use and improve the quality of life of patients.

Acknowledgments

Supported by the Ministry of Small and Medium-Sized Enterprises and Startups, Korea, under the Regional Specialized Industry Development Program (R&D, R0003813) supervised by the Korea Institute for Advancement of Technology.

Some of the results included in this manuscript were presented at the ARVO 2019 Annual Meeting.

Disclosure: **S. Kim**, Ildong Pharmaceutical Co., Ltd. (P); **G. Min**, None; **B. Kim**, None; **D. Lee**, None; **M. Lee**, None; **J.-H. Ko**, None; **H.-S. Kwon**, Ildong Pharmaceutical Co., Ltd. (P)

References

1. Stewart MW. Clinical and differential utility of VEGF inhibitors in wet age-related macular degeneration: focus on aflibercept. *Clin Ophthalmol*. 2012;6:1175–1186.
2. Pennington KL, DeAngelis MM. Epidemiology of age-related macular degeneration (AMD): associations with cardiovascular disease phenotypes and lipid factors. *Eye Vis (Lond)*. 2016;3(1):34.
3. Chong V. Ranibizumab for the treatment of wet AMD: a summary of real-world studies. *Eye (Lond)*. 2016;30(2):270–286.
4. Yang S, Zhao J, Sun X. Resistance to anti-VEGF therapy in neovascular age-related macular degeneration: a comprehensive review. *Drug Des Devel Ther*. 2016;10:1857–1867.
5. Guo H-F, Vander Kooi CW. Neuropilin functions as an essential cell surface receptor. *J Biol Chem*. 2015;290(49):29120–29126.
6. Maj E, Papiernik D, Wietrzyk J. Antiangiogenic cancer treatment: the great discovery and greater complexity (review). *Int J Oncol*. 2016;49(5):1773–1784.
7. Koch S, van Meeteren LA, Morin E. NRP1 presented in trans to the endothelium arrests VEGFR2 endocytosis, preventing angiogenic signaling and tumor initiation. *Dev Cell*. 2014;28(6):633–646.
8. Prud'homme GJ, Glinka Y. Neuropilins are multifunctional coreceptors involved in tumor initiation, growth, metastasis and immunity. *Oncotarget*. 2012;3(9):921–939.
9. Grazia G, Pedro M. Neuropilin-1 as therapeutic target for malignant melanoma. *Front Oncol*. 2015;5:125.
10. Pan Q, Chanthery Y, Liang W-C, et al. Blocking neuropilin-1 function has an additive effect with anti-VEGF to inhibit tumor growth. *Cancer Cell*. 2007;11(1):53–67.
11. Shin T-H, Sung E-S, Kim Y-J, et al. Enhancement of the tumor penetration of monoclonal antibody by fusion of a neuropilin-targeting peptide improves the antitumor efficacy. *Mol Cancer Ther*. 2014;13(3):651–661.
12. Kang H-J, Kim H-J, Jung M-S, Han JK, Cha SH. Optimal expression of a Fab-effector fusion protein in *Escherichia coli* by removing the cysteine residues responsible for an interchain disulfide bond of a Fab molecule. *Immunol Lett*. 2017;184:34–42.
13. Smith LE, Wesolowski E, McLellan A, et al. Oxygen-induced retinopathy in the mouse. *Invest Ophthalmol Vis Sci*. 1994;35(1):101–111.
14. Sumner G, Georgaros C, Rafique A, et al. Anti-VEGF drug interference with VEGF quantitation in the R&D systems human quantikine VEGF ELISA kit. *Bioanalysis*. 2019;11(5):381–392.
15. Regula JT, Lundh von Leithner P, Foxton R, et al. Targeting key angiogenic pathways with a

translational vision science & technology

Downloaded from hwmaint.iovs.org on 04/25/2024

bispecific crossMAB optimized for neovascular eye diseases. *EMBO Mol Med*. 2016;8(11):1265–1288.
16. Papadopoulos N, Martin J, Ruan Q, et al. Binding and neutralization of vascular endothelial growth factor (VEGF) and related ligands by VEGF Trap, ranibizumab and bevacizumab. *Angiogenesis.* 2012;15(2):171–185.
17. Caroline P-M, Paul F, Ian ME, Herzog B, Jünemann-Ramírez M, Zachary IC. Neuropilin-1 mediates PDGF stimulation of vascular smooth muscle cell migration and signalling via $p130^{Cas}$. *Biochem J*. 2011;435(3):609–618.
18. Mamer SB, Chen S, Weddell JC, et al. Discovery of high-affinity PDGF-VEGFR interactions: redefining RTK dynamics. *Sci Rep*. 2017;7:16439.
19. Fernandez-Robredo P, Selvam S, Powner MB, Sim DA, Fruttiger M. Neuropilin 1 involvement in choroidal and retinal neovascularization. *PLoS One*. 2017;12(1):e0169865.
20. Gaudreault J, Fei D, Beyer JC, et al. Pharmacokinetics and retinal distribution of ranibizumab, a humanized antibody fragment directed against VEGF-A, following intravitreal administration in rabbits. *Retina.* 2007;27(9):1260–1266.
21. Holmes DIR, Zachary I. The vascular endothelial growth factor (VEGF) family: angiogenic factors in health and disease. *Genome Biol*. 2005;6(2):209.
22. Stewart MW. Aflibercept (VEGF Trap-Eye): the newest anti-VEGF drug. *Br J Ophthalmol*. 2012;96(9):1157–1158.

translational vision science & technology

Downloaded from hwmaint.iovs.org on 04/25/2024